

Charge and spin correlations of a Peierls insulator after a quench

Martin Hohenadler

Institut für Theoretische Physik und Astrophysik, Universität Würzburg, 97074 Würzburg, Germany

(Dated: April 30, 2022)

Electron-phonon coupling plays a central role for time-dependent phenomena in condensed matter, for example in photo-excitation experiments. We use the continuous-time quantum Monte Carlo method to study the real-time evolution of charge and spin correlation functions of a Peierls insulator after a quench to a noninteracting Hamiltonian. This approach gives exact results, and fully takes into account quantum phonon effects without relying on a Hilbert space truncation. It is also free from a dynamical sign problem. The observed time dependence is compared to free-fermion time evolution starting from a dimerized state. Our exact results provide a benchmark for more realistic calculations, and may be directly applicable to experiments with cold atoms or trapped ions.

PACS numbers: 71.38.-k, 71.45.Lr, 63.20.kd

I. INTRODUCTION

The enormous current interest in the time evolution or nonequilibrium behavior of quantum systems is driven by significant developments in the field of experimental physics. Of particular importance are time-resolved studies of cold atoms in optical lattices following the seminal work by Greiner *et al.*,¹ and the progress with femtosecond spectroscopy,^{2–5} including time-resolved photoemission spectroscopy.^{6,7} These methods enable researchers to carry out pump-probe experiments and to study photo-excitation and photo-induced phase transitions.^{4,8–14}

Theoretical studies are particularly difficult for systems with strong correlations, as relevant for several classes of materials. Whereas much progress has been made in developing methods to study correlated systems in equilibrium, the description of time-dependent or nonequilibrium problems is extremely challenging. As a result, it is currently not possible to reliably describe experiments. Promising directions of research include time-dependent density matrix renormalization group methods,¹⁵ extensions of quantum cluster methods such as dynamical mean-field theory^{16,17} and the variational cluster approach,¹⁸ as well as extensions of Luttinger liquid theory.¹⁹ A review of theoretical methods for correlated systems has been given by Eckstein *et al.*²⁰ An important open question for gapless one-dimensional systems is if the time dependence of generic lattice models is indeed fully captured by Luttinger liquid theory.²¹

Whereas these ideas have successfully been applied to models of interacting spins, fermions or bosons, much less is known about phenomena related to electron-phonon interaction. The latter plays a crucial role since phonons are often the fastest channel available for thermalization via scattering.²² However, the infinite bosonic Hilbert space as well as the resulting retarded electron-electron interaction pose a serious challenge to theoretical methods. Whereas exact results have been obtained for a single polaron,^{23–25} a single bipolaron,²⁶ and a single-molecule device,²⁷ lattice models with finite band fillings are much more challenging to study. Recent work along these lines makes use of the density

matrix renormalization group on small systems,²⁸ the so-called double-phonon cloud method,²⁹ restricted phonon Hilbert spaces,³⁰ as well as classical phonons.³¹

A particularly interesting class of experiments involves photo-induced phase transitions across a metal-insulator Peierls transition;^{4,8–14,32} see Ref. 33 for a review. A laser pulse excites the system out of the insulating, charge-ordered state, as visible for example from the band structure (probed by time and angle-resolved photoemission spectroscopy)¹³ or from the reflectivity.¹¹ After the photo-induced melting of charge order, the system relaxes back towards its original state. Such experiments also reveal the typically very different time scales for electron and ion dynamics. So far, a photo-induced phase transition of a Peierls system has been considered theoretically in Ref. 30 using a classical phonon approximation. Since nonlocal correlations are a defining feature of charge ordered states, local approximations such as dynamical-mean field theory are of limited use.

Motivated by the ongoing effort to improve the available theoretical tools for the study of electron-phonon systems, we consider here a quench from a Peierls insulator to noninteracting fermions by switching off the electron-phonon interaction. The model we use is the one-dimensional Holstein model. The time evolution of charge and spin correlation functions after the quench is studied with an extension of the continuous-time quantum Monte Carlo method.³⁴ Although such a quench does not fully capture the complexity encountered in pump-probe experiments, it provides us with a rare opportunity to obtain exact results for the time evolution of an electron-phonon system. Our findings can serve as a nontrivial benchmark for future numerical calculations (for example with methods that rely on a truncation of the phonon Hilbert space), and may even be relevant for experimental realizations of electron-phonon models in optical lattices^{35–38} or ion traps.^{39,40}

The paper is organized as follows. In Sec. II, we discuss the model, in Sec. III, we provide details about the method used, in Sec. IV, we present our results, and Sec. V contains our conclusions.

II. MODEL

The Peierls metal-insulator transition in one dimension can be investigated in the framework of Holstein's molecular crystal model,⁴¹ defined by the Hamiltonian

$$\hat{H} = \sum_{k\sigma} \epsilon(k) c_{k\sigma}^\dagger c_{k\sigma} + \sum_i \left(\frac{\hat{P}_i^2}{2M} + \frac{K\hat{Q}_i^2}{2} \right) - g(t) \sum_i \hat{Q}_i (\hat{n}_i - 1). \quad (1)$$

The first term, referred to as \hat{H}_0 in the following, describes nearest-neighbor hopping of electrons with the usual tight-binding band structure $\epsilon(k) = -2J \cos k$; we have set the lattice constant equal to one, and take the hopping integral as the energy unit. The second and third terms correspond to the lattice degrees of freedom and the electron-phonon coupling. The lattice is described by means of harmonic oscillators with frequency $\omega_0 = \sqrt{K/M}$, displacement \hat{Q}_i and momentum \hat{P}_i , and the coupling is of the density-displacement type proposed by Holstein;⁴¹ $g(t)$ is the coupling constant. We use the usual definitions $\hat{n}_{i\sigma} = c_{i\sigma}^\dagger c_{i\sigma}$, $\hat{n}_i = \sum_\sigma \hat{n}_{i\sigma}$, and $n = \langle \hat{n}_i \rangle$. A useful dimensionless coupling parameter is given by the ratio $\lambda = 2\varepsilon_p/W$, where $\varepsilon_p = g^2/2K$ is the polaron binding energy, and $W = 4J$ is the bare bandwidth. We consider a half filled band, *i.e.*, $\langle \hat{n}_i \rangle = 1$.

As discussed in Sec. I, we study a quantum quench to a noninteracting Hamiltonian. This is achieved by a time-dependent coupling constant $g(t)$. Explicitly, we take

$$g(t) = \begin{cases} g, & t = 0, \\ 0, & t > 0. \end{cases} \quad (2)$$

Because there is no coupling between electrons and the lattice after such a quench, the time evolution will be determined by the hopping term \hat{H}_0 only.

III. METHOD

The continuous-time quantum Monte Carlo (CTQMC) method is based on a weak-coupling Dyson expansion of the path integral for the partition function.³⁴ For finite systems, all possible vertex contributions can be summed stochastically, thereby giving exact results with only statistical errors. The CTQMC method has been used quite extensively for lattice and impurity problems, see Ref. 42 for a review. Because it is formulated in terms of an action, the CTQMC method permits us to simulate models with retarded interactions, which arise in the path integral for electron-phonon models when integrating analytically over the lattice degrees of freedom.⁴³ This approach has been applied to study a variety of electron-phonon models;^{44–48} numerical details can be found in Ref. 47. Because the method relies on an analytical integration

over the phonon degrees of freedom, lattice properties such as local displacements cannot be directly measured.

Quantum Monte Carlo simulations of time-dependent problems are inherently limited by the dynamical sign problem related to the time evolution operator $\exp(i\hat{H}t)$. Progress has been made by considering simplified situations where the sign problem can be avoided or limited, including quantum quenches to noninteracting systems,⁴⁹ and studies of (effective) impurity problems. For the CTQMC method, the first application to a nonequilibrium problem involving phonons was achieved in Ref. 50, and a review of previous work is found in Ref. 42. Recently, the weak-coupling CTQMC method was formulated on the Keldysh contour.⁴⁹

In principle, the method of Ref. 49 can be extended to a retarded electron-electron interaction. The resulting algorithm would, in principle, be suitable to study rather general problems, but with the usual limitation to short times due to the dynamical sign problem.⁴⁹ Here, by applying ideas from previous work using auxiliary-field methods,⁴⁹ we focus on quenches to noninteracting systems. In simulations of the time evolution *after* the electron-phonon coupling g has been switched off [see Eq. (2)], interaction vertices are restricted to imaginary times on the Keldysh contour, and there is no dynamical sign problem.

The numerical method proceeds as follows. The interacting Holstein model (1) is simulated with the CTQMC method using standard Monte Carlo updates (addition and removal of vertices, flipping of Ising spins⁴³) to obtain configurations reflecting the initial, correlated state at time $t = 0$. The interacting single-particle Green's function matrix at equal imaginary times,

$$[\mathbf{G}_\sigma(t=0)]_{ij} = \langle c_{i\sigma} c_{j\sigma}^\dagger \rangle, \quad (3)$$

is calculated for a given vertex configuration from the Dyson equation.^{34,43} From $\mathbf{G}_\sigma(t=0)$, all relevant correlation functions and observables at $t = 0$ can be obtained using Wick's theorem.^{34,43} For quenches of the form (2), expectation values at times $t > 0$ follow from the time-propagated Green's function

$$\mathbf{G}_\sigma(t) = e^{-i\hat{H}_0 t} \mathbf{G}_\sigma(t=0) e^{i\hat{H}_0 t}, \quad (4)$$

in combination with Wick's theorem. The additional numerical effort compared to a time-independent simulation amounts to the evaluation of Eq. (4) and of observables of interest for each value of t . Results for each t are averaged over different Monte Carlo configurations. Whereas equal-time observables can easily be calculated in this way, time-displaced correlation functions require a formulation on the full Keldysh contour.

IV. RESULTS

For a half-filled band, the Holstein model (1) describes a transition from a metal to a Peierls insulator driven

by the electron-phonon interaction. At $T = 0$, the Peierls state has long-range charge order with wavevector $q = 2k_F$, and a gap in the single-particle spectrum.⁵¹ In addition, a spin gap presumably exists for any nonzero electron-phonon interaction, as a result of electrons pairing into singlets.⁴⁷ Whereas the model is dimerized and insulating for any $\lambda > 0$ in the mean-field limit $\omega_0 = 0$,⁵¹ numerical results^{52–55} indicate a nonzero critical value for $\omega_0 > 0$ as a result of quantum lattice fluctuations. For an overview of previous work, see Ref. 47.

Here, we consider parameters for which Hamiltonian (1) is in the insulating Peierls phase. Explicitly, we take $\lambda = 0.5$, and two values of the phonon frequency, $\omega_0 = 0.5J$, and $5J$. According to quantum Monte Carlo results,⁵⁵ $\lambda = 0.5$ is well inside the ordered phase for $\omega_0 = 0.5J$ (the critical coupling is about 0.25), and just above the critical coupling for $\omega_0 = 5J$. Since our simulations are carried out at a low but finite temperature, the system will be in a thermal initial state before the quench. However, the results shown below are practically identical for $\beta J = L$ and $\beta J = 2L$.

Among the equal-time observables accessible with the present method, the real-space charge and spin correlation functions

$$\begin{aligned} S_\rho(r) &= \langle \hat{n}_r \hat{n}_0 \rangle, \\ S_\sigma(r) &= \langle \hat{S}_r^z \hat{S}_0^z \rangle, \end{aligned} \quad (5)$$

are of particular interest. Since we consider a quench to the noninteracting Hamiltonian \hat{H}_0 , we compare the correlation functions to those of free fermions, which have the form⁵⁶

$$S_\rho(r) = S_\sigma(r) = -\frac{1}{(\pi r)^2} + \frac{C}{r^2} \cos(2k_F r). \quad (6)$$

Here, we have set $K_\rho = K_\sigma = 1$, as appropriate for free fermions. In contrast, the Peierls state is formally described by $K_\rho = 0$ (implying long-range $2k_F$ charge order) and $K_\sigma = 0$ (reflecting the spin gap which leads to exponentially suppressed spin correlations).⁴⁷

Figure 1 shows results for $S_\rho(r)$ at different times t for $\omega_0 = 0.5J$ and $\lambda = 0.5$, as calculated from the time-dependent Green's function (4). Panels (a)–(d) correspond to different times tJ in the interval $[0, 0.7]$, whereas panel (e) shows a closeup. Full lines show the charge correlation function at time t after the quench, whereas dotted lines are results for free fermions obtained numerically.

We first consider the short-time behavior. At $t = 0$, Fig. 1(a), we observe the clear $2k_F$ charge correlations expected for the Peierls state. At $t > 0$, after the quench to $\lambda = 0$, these oscillations decay over a time scale of about $J/\sqrt{2}$. For t close to this value, $2k_F$ oscillations are practically absent at large distances. Shortly before that time, namely for $tJ \approx 0.63$, small-amplitude $2k_F$ oscillations comparable to the free-fermion results are visible, see Fig. 1(e). Whereas the charge correlations for $tJ = 0.7$ in Fig. 1(d) agree well with those for the noninteracting system on the scale of the figure, the closeup

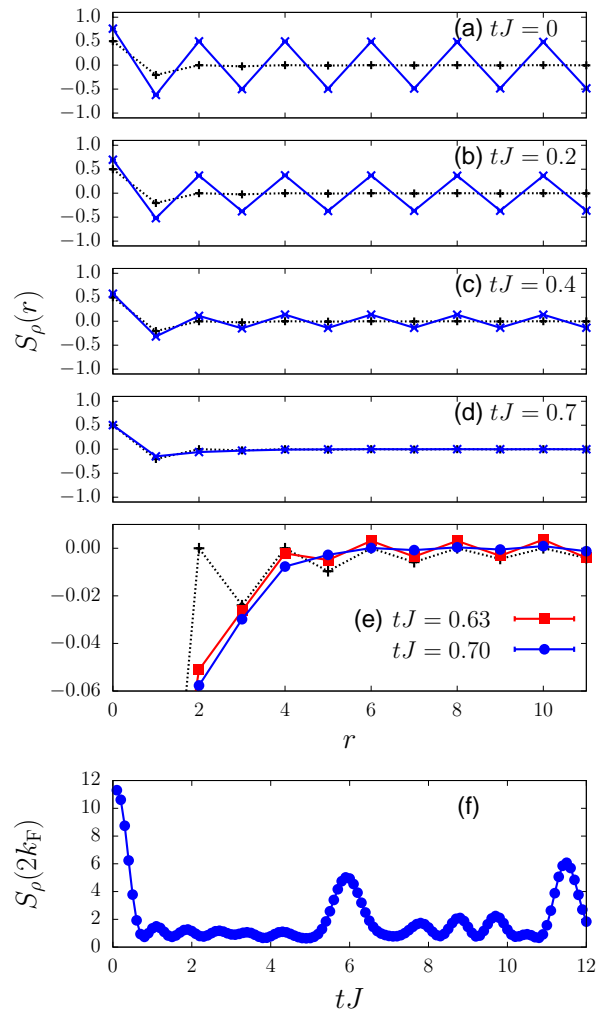


FIG. 1. (Color online) Real-space charge correlations $S_\rho(r)$ (full lines) at different times t after the quench. Here, $\lambda = 0.5$, $\omega_0 = 0.5J$, $L = 22$ and $\beta J = 44$. Dotted lines correspond to $S_\rho(r)$ for $\lambda = 0$. Panel (e) shows a closeup of panel (d), and additional results for $tJ = 0.63$. (f) Time evolution of the amplitude for $q = 2k_F$ charge correlations.

in Fig. 1(e) reveals that noticeable differences remain at small distances even for the “optimal time” of $tJ = 0.63$, which may be expected in the absence of real thermalization in an integrable system.

The results for the charge structure factor $S_\rho(q)$ (the Fourier transform of the real-space charge correlator) at $q = 2k_F$, shown in Fig. 1(f), again illustrate the time scale $tJ \approx 0.7$ for the initial decay, as well as oscillations and partial revivals at larger times. A detailed discussion of revivals will be given below for the case of the double occupation, which shows the same overall features.

Figure 2 shows the corresponding results for the spin correlation function $S_\sigma(r)$. The times shown are the same as in Fig. 1. In contrast to $S_\rho(r)$, Fig. 1(a), there are no discernible $2k_F$ correlations at $t = 0$, in accordance with the nonzero spin gap of the Peierls state. After the

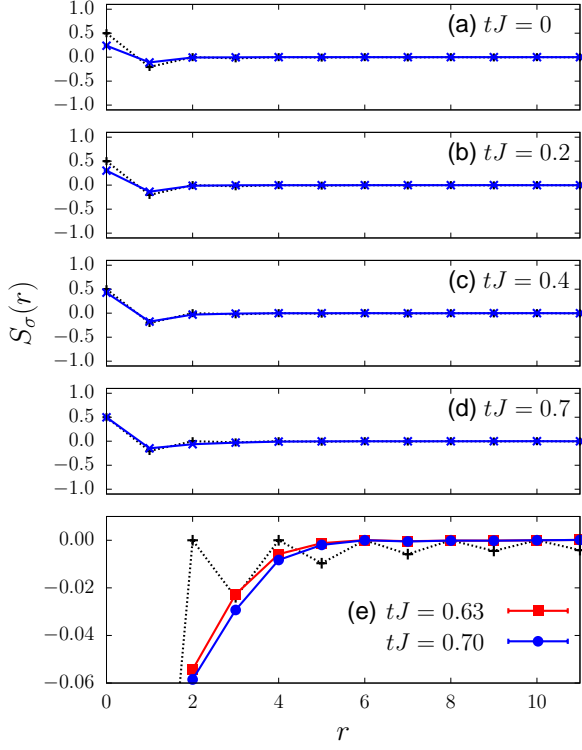


FIG. 2. (Color online) Real-space spin correlations $S_\sigma(r)$ (full lines) at different times t after the quench. Here, $\lambda = 0.5$, $\omega_0 = 0.5J$, $L = 22$ and $\beta J = 44$. Dotted lines correspond to $S_\sigma(r)$ for $\lambda = 0$. Panel (e) shows a closeup of panel (d), and additional results for $tJ = 0.63$.

quench, the deviations from the noninteracting results visible at short distances diminish as a function of time. For $tJ = 0.7$, similar to the charge correlations, $S_\sigma(r)$ looks very similar to the free-fermion result on the scale of Fig. 2(d), but the closeup in Fig. 2(e) again reveals clear differences at small distances. Interestingly, the results for $S_\sigma(r)$ in Fig. 2(e) agree within the symbol size used with those for $S_\rho(r)$ in Fig. 1(e), despite substantial differences at $t = 0$.

Because the system is quenched to a noninteracting and hence integrable Hamiltonian \hat{H}_0 , real thermalization is not possible.⁵⁷ Instead, the time evolution seen in Figs. 1 and 2 is related to dephasing. Conserved quantities such as the total energy and the momentum distribution function are independent of t . Because the time evolution is determined by \hat{H}_0 , it is independent of the electron-phonon parameters λ and ω_0 . However, the values of these parameters do modify the initial state and hence have an impact on results at $t > 0$. As emphasized before, our method fully accounts for quantum phonon (and thermal) fluctuations in the initial state. Most importantly, an increase of the phonon frequency brings the initial state closer to the Peierls phase boundary.⁵⁵

To illustrate the dependence of charge order and its time evolution on the phonon frequency, we show in Fig. 3(a) the double occupancy, $\langle n_{i\uparrow}n_{i\downarrow} \rangle$, which reflects

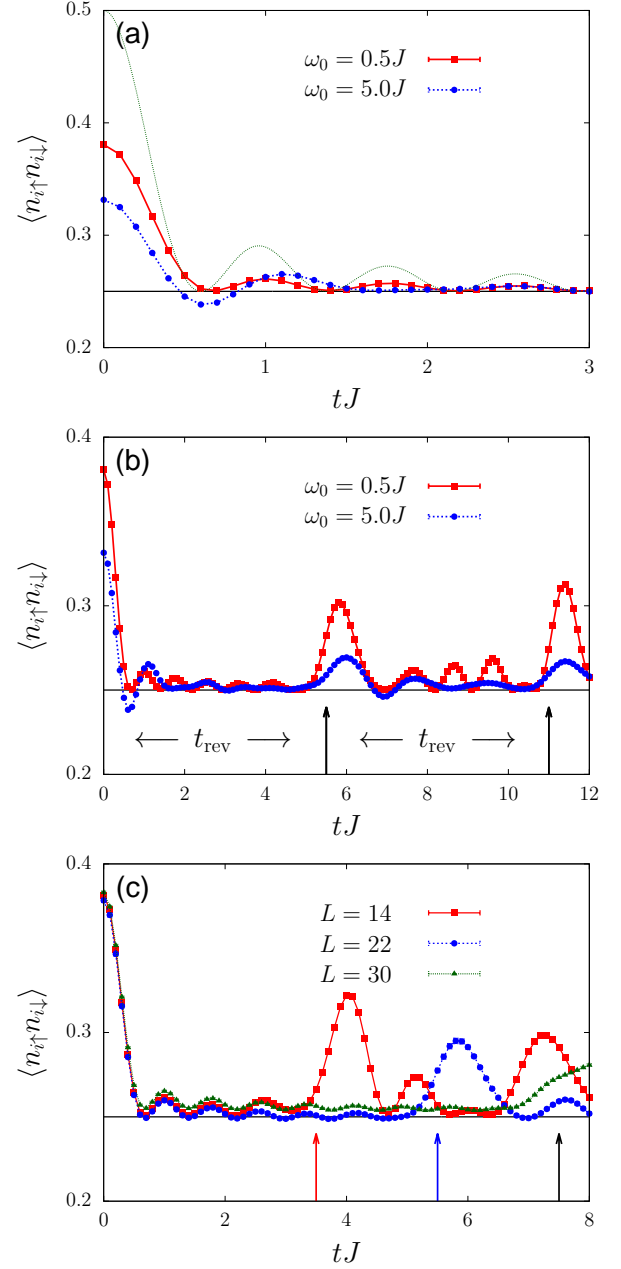


FIG. 3. (Color online) Double occupancy as a function of time at fixed $\lambda = 0.5$. (a) Short-time behavior for two different phonon frequencies at $L = 22$ and $\beta J = 44$. The dotted line corresponds to the free-fermion result, see text, and the vertical line to the value 0.25. (b) As in (a) but showing a larger time interval. Arrows indicate the first two periods of the revival time $t_{\text{rev}}J = L/4$. (c) Results for different system sizes for $\omega_0 = 0.5J$ and $\beta J = L$. Arrows indicate t_{rev} .

the pairing of electrons at the same site in the Peierls state, and its decay after the quench. Comparing the cases of $\omega_0 = 0.5J$ and $\omega_0 = 5J$, Fig. 3(a) reveals a significantly smaller double occupancy at $t = 0$ for $\omega_0 = 5J$ than for $\omega_0 = 0.5J$. At $t > 0$, we observe a fast initial decay of the double occupancy toward the noninteract-

ing value 0.25. The time scale is the same as that for the decay of $2k_F$ charge correlations in Fig. 1(f). After the first minimum, oscillations with a frequency $\sim 0.5/J$ occur, and the double occupation approaches 0.25.

To better understand these results, we also include in Fig. 3(a) the result for the decay of the double occupation in a free-fermion model, with an initial state corresponding to a perfect alternation of empty and doubly occupied sites, $|\Psi_{\text{CDW}}\rangle = \prod_i c_{2i\uparrow}^\dagger c_{2i\downarrow}^\dagger |0\rangle$.⁵⁸ This state may be regarded as a perfectly dimerized, mean-field Peierls state. The time evolution of the double occupation starting from $|\Psi_{\text{CDW}}\rangle$ is given by⁵⁸ $\langle \hat{n}_{i\uparrow} \hat{n}_{i\downarrow} \rangle = \frac{1}{4} [1 + J_0^2(4tJ)]$, where J_0 is the Bessel function of the first kind. Starting from the value 0.5 corresponding to full dimerization at $t = 0$, the double occupation decays toward 0.25, showing several periods of oscillation. This behavior is very similar to the results for the Holstein model, and the time scale for the initial decay agrees quite well, suggesting that the latter is related to the noninteracting Hamiltonian. The double occupation always stays above the noninteracting value 0.25 in the free-fermion results. Whereas the same is true for the data for $\omega_0 = 0.5J$ in Fig. 3(a), the results for $\omega_0 = 5J$ fall below 0.25 at short times. A possible explanation for this difference is that the case of $\omega_0 = 0.5J$ is closer to the mean-field limit $\omega_0 = 0$. Finally, whereas the height of consecutive maxima decreases monotonically for free fermions, this is not the case for the Holstein model (the fourth maximum is higher than the third for $\omega_0 = 5J$). We attribute these differences to correlations in the initial state of the Holstein model.

At larger times, shown in Fig. 3(b), we observe partial revivals of the double occupation. The time between such revivals, t_{rev} , is constant and independent of the initial state, as seen in Fig. 3(b). This observation can be explained in terms of the findings of Ref. 59; the revival time of an integrable system after a quench is⁵⁹

$$t_{\text{rev}} \approx \frac{L}{2v_{\text{max}}}, \quad (7)$$

where v_{max} is the maximal velocity, in our case given by $v_{\text{max}} = \max|\partial\epsilon(k)/\partial k| = 2J$. Physically, v_{max} is the maximum velocity for the propagation of information after the quench. Using the result for v_{max} , we expect $t_{\text{rev}} = L/4J = 5.5$, in very good agreement with the revivals visible in Fig. 3(a). To further verify the validity of Eq. (7), we show in Fig. 3(b) the double occupation as a function of time for three different system sizes L . Again, the estimate $t_{\text{rev}} = L/4J$ agrees well with the onset of the first revival. The same revival times can also be identified in the results for the charge correlations shown in

Fig. 1(f). Our observations are thus in agreement with the general statement in Ref. 59 that the revival time does not depend on the initial state if the Hamiltonian is local, see also Ref. 60.

V. CONCLUSIONS

Motivated by an increasing number of experiments on ultrafast dynamics after photo-induced phase transitions, and by the enormous challenge of numerically describing time-dependent phenomena in systems with electron-phonon interaction, we considered the quench of a Peierls insulator to a noninteracting Hamiltonian. Using an extension of the continuous-time quantum Monte Carlo method, we presented exact results for equal-time charge and spin correlation functions. The time evolution of the latter is related to dephasing, and we find that the dominant $2k_F$ charge correlations of the initial Peierls state decay over a time scale of about $J/\sqrt{2}$. In the absence of thermalization, differences to the correlation functions of free fermions remain. At longer times, we observe partial revivals, with revival times that depend on the maximal velocity and system size.

In the present case, the electron-phonon coupling and the quantum nature of phonons only play a role for the initial state. Increasing (decreasing) the phonon frequency (the coupling) moves the system closer to the metallic state, thereby suppressing charge order. Importantly, the results shown cannot be obtained by considering the antiadiabatic limit $\omega_0 \rightarrow \infty$, where the Holstein model maps onto an attractive Hubbard model. The reason is that the attractive Hubbard model at half filling always remains metallic, with the Luttinger liquid parameter K_ρ fixed to one by symmetry.⁶¹

The exact results presented here can serve as benchmarks for more realistic calculations using, for example, the density-matrix renormalization group. In the latter, the phonon Hilbert space has to be truncated for the initial state as well as for the time evolution. Finally, our findings may even become directly relevant for experiments with cold atoms or trapped ions; several different proposals exist how to realize electron-phonon Hamiltonians in such systems.^{35–37,39,40}

ACKNOWLEDGMENTS

Computer time at the Jülich Supercomputing Centre, support from the DFG Grant No. Ho 4489/2-1 (Forschergruppe FOR 1807), and discussions with F. F. Assaad, F. Goth, and M. Sentef are gratefully acknowledged.

¹ M. Greiner, O. Mandel, T. Esslinger, T. W. Hänsch, and I. Bloch, *Nature (London)* **415**, 39 (2002)

² A. Pashkin, M. Porer, M. Beyer, K. W. Kim, A. Dubroka,

C. Bernhard, X. Yao, Y. Dagan, R. Hackl, A. Erb, J. Demsar, R. Huber, and A. Leitenstorfer, *Phys. Rev. Lett.* **105**, 067001 (2010)

- ³ C. Gadermaier, A. S. Alexandrov, V. V. Kabanov, P. Kusar, T. Mertelj, X. Yao, C. Manzoni, D. Brida, G. Cerullo, and D. Mihailovic, *Phys. Rev. Lett.* **105**, 257001 (2010)
- ⁴ Y. Kawakami, T. Fukatsu, Y. Sakurai, H. Unno, H. Itoh, S. Iwai, T. Sasaki, K. Yamamoto, K. Yakushi, and K. Yonemitsu, *Phys. Rev. Lett.* **105**, 246402 (2010)
- ⁵ S. Wall, D. Brida, S. R. Clark, H. P. Ehrke, D. Jaksch, A. Ardavan, S. Bonora, H. Uemura, Y. Takahashi, T. Hasegawa, H. Okamoto, G. Cerullo, and A. Cavalleri, *Nature Phys.* **7**, 114 (2011)
- ⁶ L. Perfetti, P. A. Loukakos, M. Lisowski, U. Bovensiepen, H. Eisaki, and M. Wolf, *Phys. Rev. Lett.* **99**, 197001 (2007)
- ⁷ R. Cortés, L. Rettig, Y. Yoshida, H. Eisaki, M. Wolf, and U. Bovensiepen, *Phys. Rev. Lett.* **107**, 097002 (2011)
- ⁸ M. Chollet, L. Guerin, N. Uchida, S. Fukaya, H. Shimoda, T. Ishikawa, K. Matsuda, T. Hasegawa, A. Ota, H. Yamochi, G. Saito, R. Tazaki, S.-i. Adachi, and S.-y. Koshihara, *Science* **307**, 86 (2005)
- ⁹ S. Iwai, K. Yamamoto, A. Kashiwazaki, F. Hiramatsu, H. Nakaya, Y. Kawakami, K. Yakushi, H. Okamoto, H. Mori, and Y. Nishio, *Phys. Rev. Lett.* **98**, 097402 (2007)
- ¹⁰ C. Kübler, H. Ehrke, R. Huber, R. Lopez, A. Halabica, R. F. Haglund, and A. Leitenstorfer, *Phys. Rev. Lett.* **99**, 116401 (2007)
- ¹¹ A. Tomeljak, H. Schäfer, D. Städter, M. Beyer, K. Biljakovic, and J. Demsar, *Phys. Rev. Lett.* **102**, 066404 (2009)
- ¹² S. Hellmann, M. Beye, C. Sohrt, T. Rohwer, F. Sorgenfrei, H. Redlin, M. Kalläne, M. Marczyński-Bühlöw, F. Hennies, M. Bauer, A. Föhlich, L. Kipp, W. Wurth, and K. Rossnagel, *Phys. Rev. Lett.* **105**, 187401 (2010)
- ¹³ R. G. Moore, V. Brouet, R. He, D. H. Lu, N. Ru, J.-H. Chu, I. R. Fisher, and Z.-X. Shen, *Phys. Rev. B* **81**, 073102 (2010)
- ¹⁴ S. Miyashita, Y. Tanaka, S. Iwai, and K. Yonemitsu, *J. Phys. Soc. Jpn.* **79**, 034708 (2010)
- ¹⁵ U. Schollwöck, *Annals of Physics* **326**, 96 (2011)
- ¹⁶ P. Schmidt and H. Monien, *cond-mat/0202046*
- ¹⁷ J. K. Freericks, V. M. Turkowski, and V. Zlatić, *Phys. Rev. Lett.* **97**, 266408 (2006)
- ¹⁸ M. Knap, W. von der Linden, and E. Arrigoni, *Phys. Rev. B* **84**, 115145 (2011)
- ¹⁹ C. Karrasch, J. Rentrop, D. Schuricht, and V. Meden, *Phys. Rev. Lett.* **109**, 126406 (2012)
- ²⁰ M. Eckstein, A. Hackl, S. Kehrein, M. Kollar, M. Moeckel, P. Werner, and F. Wolf, *Eur. Phys. J. Special Topics* **180**, 217 (2009)
- ²¹ E. Coira, F. Becca, and A. Parola, *Eur. Phys. J. B* **86**, 55 (2013)
- ²² M. Sentef, A. F. Kemper, B. Moritz, J. K. Freericks, Z.-X. Shen, and T. P. Devereaux, *arXiv:1212.4841*(2012)
- ²³ D. Golež, J. Bonča, L. Vidmar, and S. A. Trugman, *Phys. Rev. Lett.* **109**, 236402 (2012)
- ²⁴ L.-C. Ku and S. A. Trugman, *Phys. Rev. B* **75**, 014307 (2007)
- ²⁵ H. Fehske, G. Wellein, and A. R. Bishop, *Phys. Rev. B* **83**, 075104 (2011)
- ²⁶ D. Golež, J. Bonča, and L. Vidmar, *Phys. Rev. B* **85**, 144304 (2012)
- ²⁷ Y. Vinkler, A. Schiller, and N. Andrei, *Phys. Rev. B* **85**, 035411 (2012)
- ²⁸ H. Matsueda, S. Sota, T. Tohyama, and S. Maekawa, *J. Phys. Soc. Jpn.* **81**, 013701 (2012)
- ²⁹ G. De Filippis, V. Cataudella, E. A. Nowadnick, T. P. Devereaux, A. S. Mishchenko, and N. Nagaosa, *Phys. Rev. Lett.* **109**, 176402 (2012)
- ³⁰ J. D. Lee, P. Moon, and M. Hase, *Phys. Rev. B* **84**, 195109 (2011)
- ³¹ K. Yonemitsu and N. Maeshima, *Phys. Rev. B* **79**, 125118 (2009)
- ³² F. Schmitt, P. S. Kirchmann, U. Bovensiepen, R. G. Moore, L. Rettig, M. Krenz, J.-H. Chu, N. Ru, L. Perfetti, D. H. Lu, M. Wolf, I. R. Fisher, and Z.-X. Shen, *Science* **321**, 1649 (2008)
- ³³ K. Yonemitsu and K. Nasu, *Phys. Rep.* **465**, 1 (2008)
- ³⁴ A. N. Rubtsov, V. V. Savkin, and A. I. Lichtenstein, *Phys. Rev. B* **72**, 035122 (2005)
- ³⁵ F. Herrera and R. V. Krems, *Phys. Rev. A* **84**, 051401 (2011)
- ³⁶ J. P. Hague and C. McCormick, *New Journal of Physics* **14**, 033019 (2012)
- ³⁷ E. Pazy and A. Vardi, *Phys. Rev. A* **72**, 033609 (2005)
- ³⁸ M. Atala, M. Aidelsburger, J. T. Barreiro, D. Abanin, T. Kitagawa, E. Demler, and I. Bloch, *arXiv:1212.0572*
- ³⁹ A. Mezzacapo, J. Casanova, L. Lamata, and E. Solano, *Phys. Rev. Lett.* **109**, 200501 (2012)
- ⁴⁰ V. M. Stojanović, T. Shi, C. Bruder, and J. I. Cirac, *Phys. Rev. Lett.* **109**, 250501 (2012)
- ⁴¹ T. Holstein, *Ann. Phys. (N.Y.)* **8**, 325; **8**, 343 (1959)
- ⁴² E. Gull, A. J. Millis, A. I. Lichtenstein, A. N. Rubtsov, M. Troyer, and P. Werner, *Rev. Mod. Phys.* **83**, 349 (2011)
- ⁴³ F. F. Assaad and T. C. Lang, *Phys. Rev. B* **76**, 035116 (2007)
- ⁴⁴ M. Hohenadler, H. Fehske, and F. F. Assaad, *Phys. Rev. B* **83**, 115105 (2011)
- ⁴⁵ F. F. Assaad, *Phys. Rev. B* **78**, 155124 (2008)
- ⁴⁶ M. Hohenadler and F. F. Assaad, *J. Phys.: Condens. Matter* **25**, 014005 (2013)
- ⁴⁷ M. Hohenadler and F. F. Assaad, *Phys. Rev. B* **87**, 075149 (2013)
- ⁴⁸ M. Hohenadler, F. F. Assaad, and H. Fehske, *Phys. Rev. Lett.* **109**, 116407 (2012)
- ⁴⁹ F. Goth and F. F. Assaad, *Phys. Rev. B* **85**, 085129 (2012)
- ⁵⁰ L. Mühlbacher and E. Rabani, *Phys. Rev. Lett.* **100**, 176403 (2008)
- ⁵¹ J. E. Hirsch and E. Fradkin, *Phys. Rev. B* **27**, 4302 (1983)
- ⁵² E. Jeckelmann, C. Zhang, and S. R. White, *Phys. Rev. B* **60**, 7950 (1999)
- ⁵³ H. Fehske, G. Hager, and E. Jeckelmann, *Europhys. Lett.* **84**, 57001 (2008)
- ⁵⁴ R. T. Clay and R. P. Hardikar, *Phys. Rev. Lett.* **95**, 096401 (2005)
- ⁵⁵ R. P. Hardikar and R. T. Clay, *Phys. Rev. B* **75**, 245103 (2007)
- ⁵⁶ H. J. Schulz, *Phys. Rev. Lett.* **64**, 2831 (1990)
- ⁵⁷ M. Rigol, V. Dunjko, V. Yurovsky, and M. Olshanii, *Phys. Rev. Lett.* **98**, 050405 (2007)
- ⁵⁸ T. Enss and J. Sirker, *New J. Phys.* **14**, 023008 (2012)
- ⁵⁹ J. Häppölä, G. B. Halász, and A. Hamma, *Phys. Rev. A* **85**, 032114 (2012)
- ⁶⁰ E. Lieb and D. Robinson, *Comm. Math. Phys.* **28**, 251 (1972)
- ⁶¹ T. Giamarchi, *Quantum Physics in One Dimension* (Clarendon Press, Oxford, 2004)